Supporting Information

MoSx-coated NbS2 nanoflakes growth on glass carbon: an advanced electrocatalyst for the hydrogen evolution reaction

Xiaofeng Zhou,[abc†] Shi-Hsin Lin,[d] Xiulin Yang,[b] Henan Li,[e] Mohamed Nejib Hedhili,[b] Lain-Jong Li[b], Wenjing Zhang*[a] and Yumeng Shi [a*†]

[a] SZU-NUS Collaborative Innovation Center for Optoelectronic Science & Technology, Key Laboratory of Optoelectronic Devices and Systems of Ministry of Education and Guangdong Province, College of Optoelectronic Engineering, Shenzhen University, Shenzhen 518060, China
[b] KAUST Catalysis Center, Physical Sciences and Engineering Division, King Abdullah University of Science and Technology, Thuwal 23955-6900, Kingdom of Saudi Arabia
[c] Shenzhen Chang Long Technology Co., Ltd., Shenzhen 518060, China
[d] Department of Materials and Optoelectronic Science, National Sun Yat-Sen University, Kaohsiung, 80424, Taiwan
[e] College of Electronic Science and Technology, Shenzhen University, Shenzhen 518060, China.

E-mail: wjzhang@szu.edu.cn & yumeng.shi@szu.edu.cn

† These authors contribute equally

Computation details

We performed first-principles calculations using Vienna ab-initio simulation package (VASP) [1,2]. Perdew-Burke-Ernzerhof (PBE) functional [3] was used throughout our calculations, with the van der Waals D2 correction [4]. We modeled hybrid materials (MoS_x@NbS_2) with a layer of defected MoS_2 with single S vacancy defects onto a layer of NbS_2, and calculate the corresponding hydrogen adsorption free energy difference Gibbs free energy (ΔG_H) [5] at the S vacancy sites. We calculated 4×4 supercells of MoS_x and MoS_x@NbS_2, using the same lattice constant of NbS_2, with a 15Å vacuum spacing. 400 eV is adopted as the energy cutoff, and 4×4×1 k-points was used. The energy convergence criteria is set to be 10^{-6} eV and the force is below 0.01 eV/Å. We considered 1, 2, 3, and 4 single S vacancy defects and the full hydrogen coverage at all defect sites on the 4×4 MoS_2.

We found that, for MoS_x ($x = 1.9375$, 1.875, 1.8125, and 1.75, respectively), ΔG_H= -0.30, -0.25, -0.36, -0.28 eV for 1-4 defects respectively. When the defected MoS_x is placed onto NbS_2, ΔG_H= -0.20, -0.25, -0.36, -0.25 eV for 1-4 defects of MoS_2 (See Figures below). ΔG is closer to zero, suggesting that the hybrid materials (MoS_x@NbS_2) render better HER performance, consistent with our experimental findings. The modulation of ΔG_H of MoS_x@NbS_2 with the defect number can be attributed to the stress for the different configurations.

For the Mo-edge sites,[6] we modeled with a 4×2 flake of MoS_2 on a 10×2 supercell of NbS_2 and compared with the pristine 4×2 flake of MoS_2. The lattice constant of NbS_2 was adopted as that of the hybrid system. With one hydrogen adsorbed (50%), the pristine MoS_2 supply a ΔG_H=-0.48 eV, while for the hybrid system, ΔG_H=-0.16 eV. The much reduced free energy difference suggests a better HER performance, which is consistent to our experimental findings.

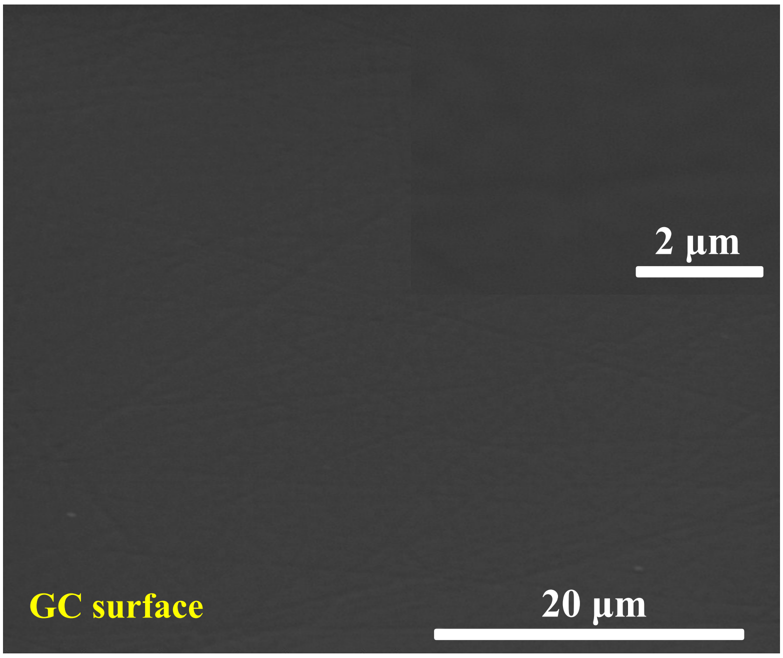

Figure S1. SEM image of the pure and polished glass carbon (GC). The inset is the corresponding higher-magnification SEM image of polished GC.

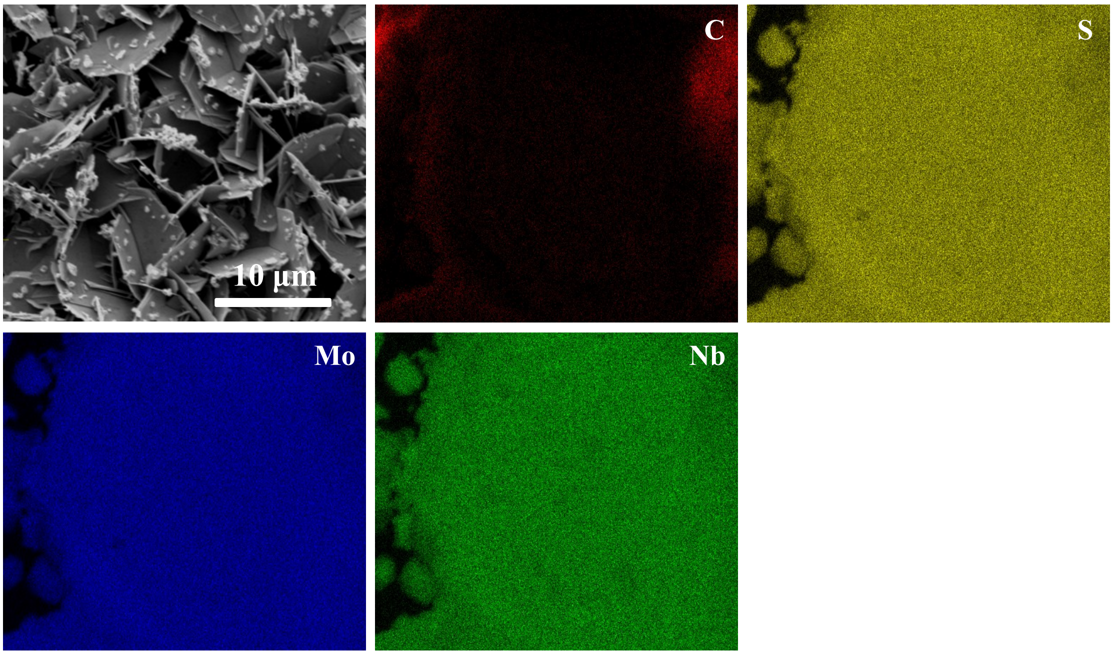

Figure S2. SEM image of $MoS_x@NbS_2/GC$ sample and the corresponding SEM element mappings.

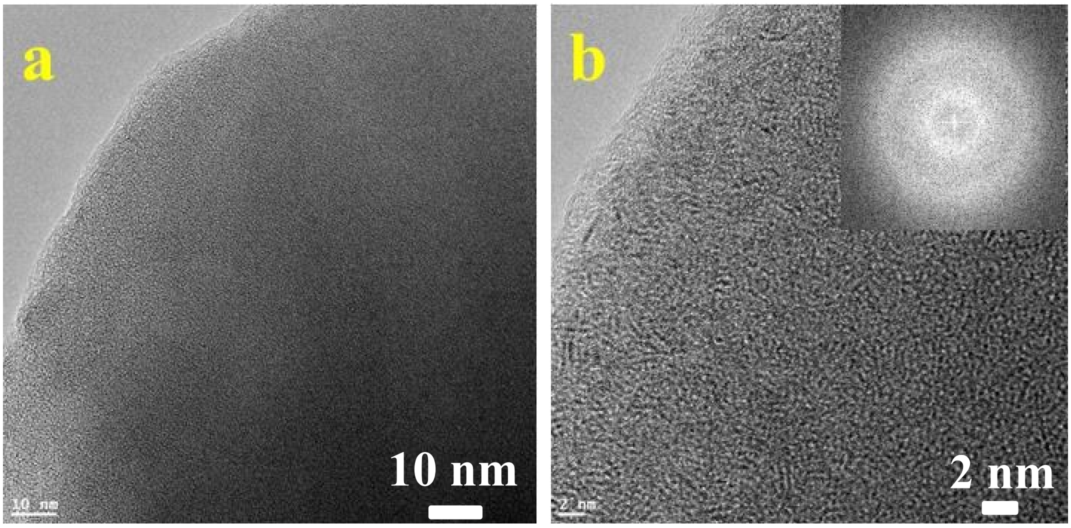

Figure S3. TEM images of MoS_x/GC with different magnifications. The inset in the right corner is the FFT data of the corresponding TEM image (b).

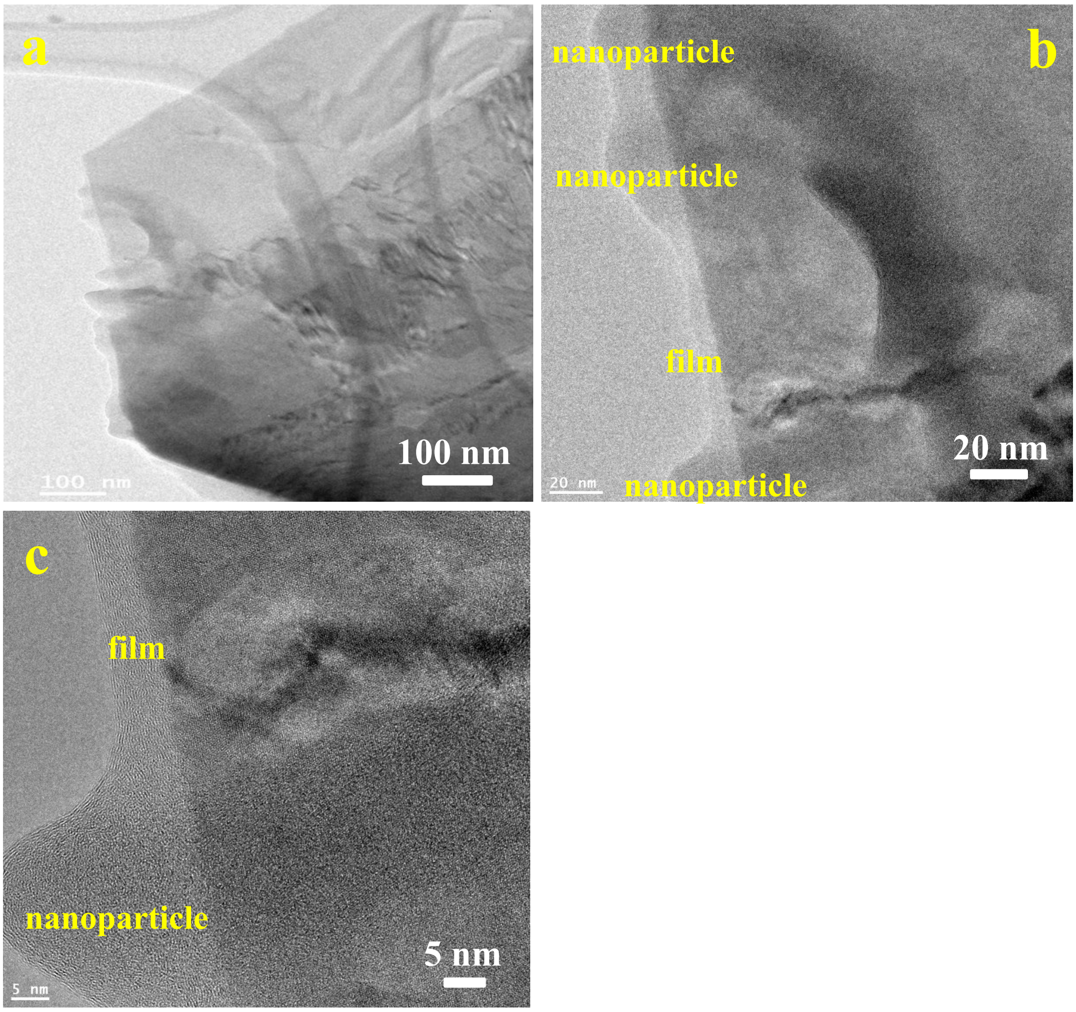

Figure S4. The more representative hybrid $MoS_x@NbS_2/GC$ TEM images with different magnifications.

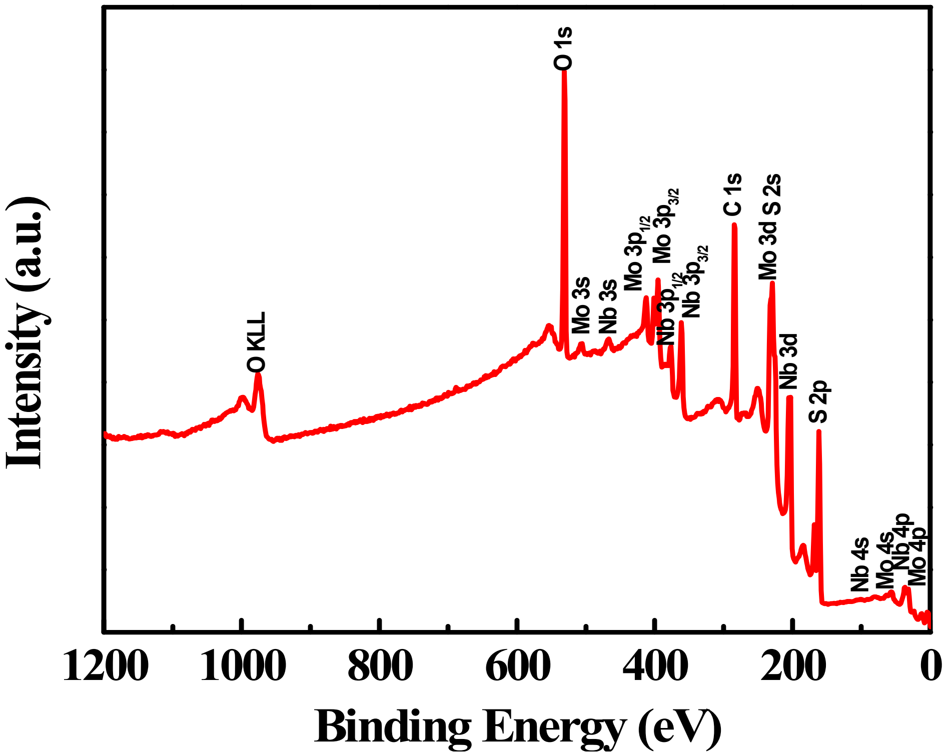

Figure S5. The XPS survey spectra of $MoS_x@NbS_2/GC$ sample.

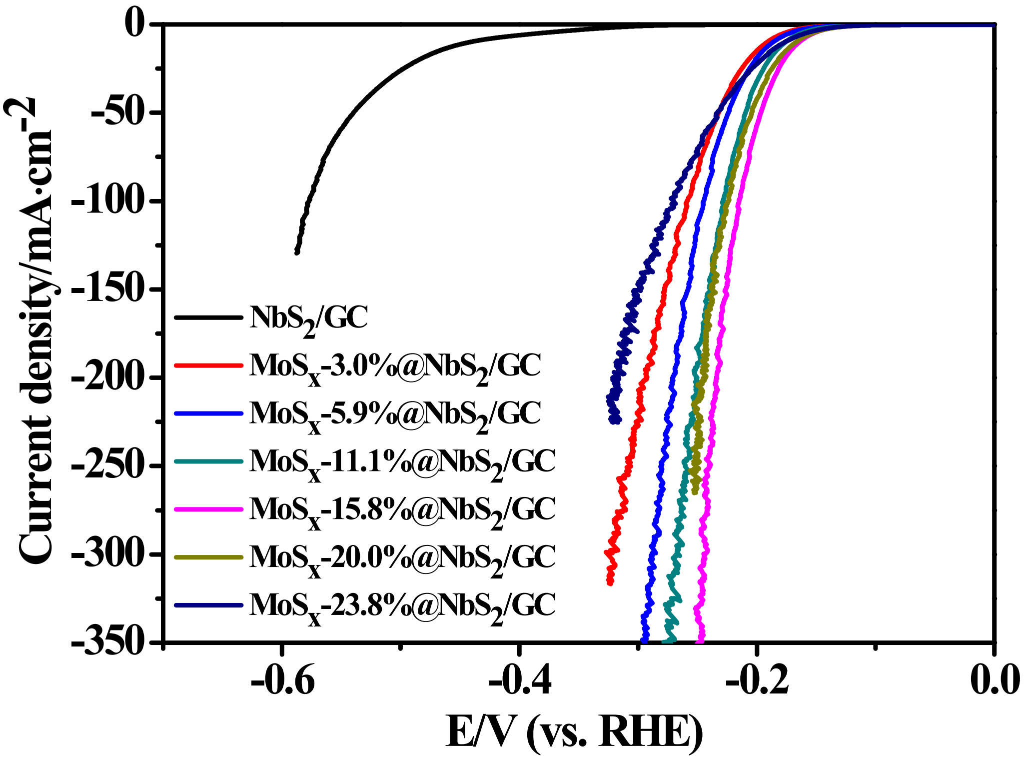

Figure S6. Polarization curves of NbS_2 (loading of 0.8 mg/cm^2) and a series of MoS_x-x@NbS_2/GC (x indicates the mass fraction of MoS_x in hybrid MoS_x@NbS_2/GC) samples with fixed amount of NbS_2 (loading of 0.8 mg/cm^2) and different drop-coating amounts of MoS_x, where the current is normalized by the geometrical area of glass carbon and the potential is after internal resistance correction.

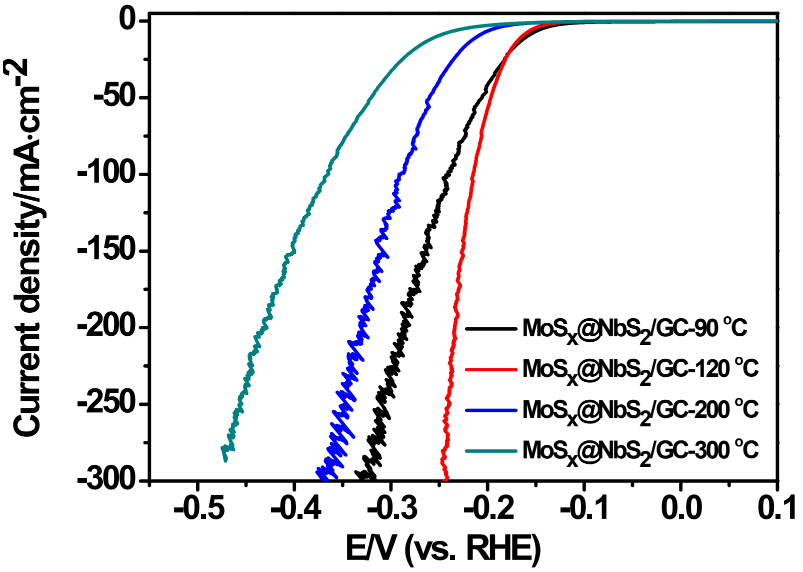

Figure S7. The Polarization curves of a series of MoS$_x$@NbS$_2$/GC (the mass fraction of MoS$_x$ in hybrid is 15.8%) samples with different annealing temperatures, where the current is normalized by the geometrical area of glass carbon and the potential is after internal resistance correction. From the Figure S6, we can clearly see that the optimum annealing temperature is 120 ^{o}C for obtaining the best HER performance of the MoS$_x$@NbS$_2$/GC catalyst.

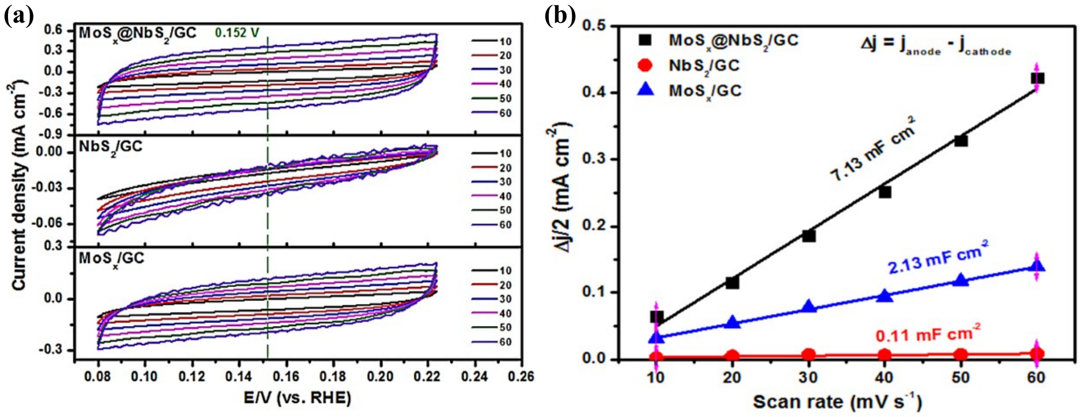

Figure S8. a) Cyclic voltammograms of three different catalysts, where the curves are taken in a potential window at various scan rates (10~60 mV s^{-1}); b) Double layer capacitance and relative electrochemically active surface area for the corresponding catalysts.

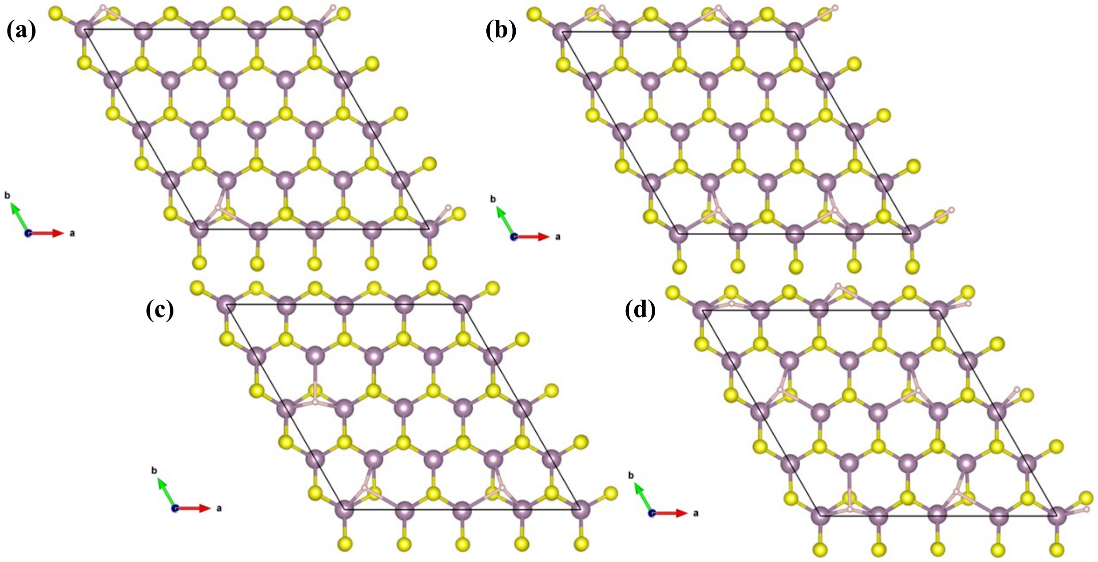

Figure S9. a) One S defect was created on a 4×4 MoS_2 supercell and one hydrogen atom can be absorbed at the defect site of the defected MoS_2 layer; b) Two S defects were created on a 4×4 MoS_2 supercell and two hydrogen atoms can be absorbed at the two defect sites of the defected MoS_2 layer; c) Three S defects were created on a 4×4 MoS_2 supercell and three hydrogen atoms can be absorbed at the three defect sites of the defected MoS_2 layer; d) Four S defects were created on a 4×4 MoS_2 supercell and four hydrogen atoms can be absorbed at the four defect sites of the defected MoS_2 layer. (hydrogen: white, Mo: purple, S: yellow).

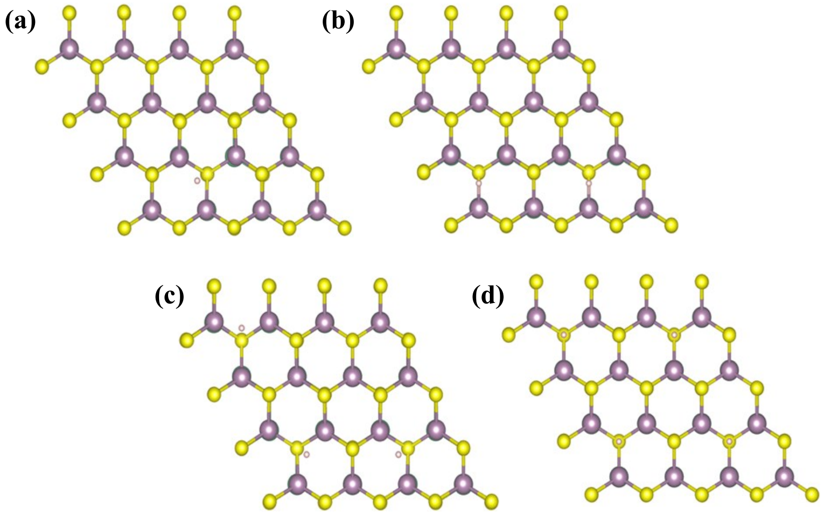

Figure S10. a) One S defect was created on a 4×4 MoS_2 supercell. One hydrogen atom can be absorbed at the defect site of the defected MoS_2 layer on top of NbS_2 layer; b) Two S defects were created on a 4×4 MoS_2 supercell. Two hydrogen atoms can be absorbed at the two defect sites of the defected MoS_2 layer on top of NbS_2 layer; c) three S defects were created on a 4×4 MoS_2 supercell. Three hydrogen atoms can be absorbed at the three defect sites of the defected MoS_2 layer on top of NbS_2 layer; d) Four S defects were created on a 4×4 MoS_2 supercell. Four hydrogen atoms can be absorbed at the four defect sites of the defected MoS_2 layer on top of NbS_2 layer. (Top view without showing the underlying NbS_2 layer; hydrogen: white, Mo: purple, S: yellow).

Table S1. Summary of HER performance for Niobium-based and molybdenum-based sulfides catalysts published recently.

Catalyst	**substrate**	**Loading amount (mg/cm^2)**	**Current density (*j*, mA/cm^2)**	**Overpotential at the corresponding *j* (mV)**	**Tafel slope (mV/dec)**	**Electrolyte Conc. (H_2SO_4)**
NbS$_2$ $^{\text{(this work)}}$	GC	0.8	-10	-442	79.2	0.5 M
MoS$_x$$^{\text{(this work)}}$	GC	0.15	-10	-221	161.9	0.5 M
MoS$_x$@NbS$_2$/GC $^{\text{(this work)}}$	GC	0.95	-10	-134	43.2	0.5 M
Co$_9$S$_8$@MoS$_2$[7]	CNFs	0.212	-10	-190	110	0.5 M
CoS$_2$@MoS$_2$ nanoarray[8]	Ti foil	---	-10	-110.5	57.3	0.5 M
MoS$_2$/CoS$_2$ nanorods[9]	CC	18.6	-10	-87	73.4	0.5 M
MoS$_2$[9]	CC	4.2	-10	-155	97.3	0.5 M
MoS$_2$/NbSe$_2$[10]	Glass carbon	---	-205	-650	79.5	0.5 M
H-NbS$_2$[11]	Glass carbon	0.01	-10	-50	30	0.5 M
NbS$_2$/rGO[12]	Glass carbon	---	-10	-500	72	0.5 M
MoS$_2$ nanoparticles[13]	CC	2.6	-25	-250	50	0.5 M
Amorphous MoS$_x$[14]	Glassy carbon	---	-10	-200	57	0.5 M
MoS$_x$/graphene/Ni foam[15]	3D Ni foams	5.01	-45	-200	42.8	0.5 M

References

[1] G. Kresse and J. Furthmüller, Phys. Rev. B **54**, 169 (1996).

[2] G. Kresse and D. Joubert, Phys. Rev. B **59**, 1758 (1999).

[3] J. P. Perdew, K. Burke and M. Ernzerhof, Phys. Rev. Lett., **77**, 3865 (1996).

[4] S. Grimme, J. Comput. Chem., **27**, 1787 (2006).

[5] J. K. Nørskov, T. Bligaard, A. Logadottir, J. R. Kitchin, J. G. Chen, S. Pandelov and U. Stimming, J. Electrochem. Soc., **152**, J23 (2005).

[6] B. Hinnemann, P. G. Moses, J. Bonde, K. P. Jørgensen, J. H. Nielsen, S. Horch, I. Chorkendorff and J. K. Nørskov, J. Am. Chem. Soc., **127**, 5308 (2005).

[7] H. Zhu, J. F. Zhang, R. P. Yanzhang, M. L. Du, Q. F. Wang, G. H. Gao, J. D. Wu, G. M. Wu, M. Zhang, B. Liu, J. M. Yao and X. W. Zhang, Adv. Mater., **27**, 4752 (2015).

[8] H. C. Zhang, Y. J. Li, T. H. Xu, J. B. Wang, Z. Y. Huo, P. B. Wan and X. M. Sun, J. Mater. Chem A, **3**, 15020 (2015).

[9] J. L. Huang, D. M. Hou, Y. C. Zhou, W. J. Zhou, G. Q. Li, Z. H. Tang, L. G. Li and S. W. Chen, J. Mater. Chem. A**, 3**, 22886 (2015).

[10] B. L. Zhao, J. Huang, Q. Fu, L. Yang, J. Y. Zhang and B. Xiang. J. Electrochem. Soc, **163**,

H384 (2016).

[11] Y. Liu, J. Wu, K. P. Hackenberg, J. Zhang, Y. M. Wang, Y. Yang, K. Keyshar, J. Gu, T. Ogitsu, R. Vajtai, J. Lou, P. M. Ajayan. B. C. Wood and B. I. Yakobson, Nat Energy, **2**, 17127 (2017).

[12] D. Gopalakrishnan, A. Lee, N. K. Thangavel and L. M. R. Arava, Sustainable Energy Fuels, **2**, 96 (2018).

[13] T. Chen, Y. H. Chang, C. L. Hsu, K. H. Wei, C. Y. Chiang, L. J. Li, Int. J. Hydrogen. Energy, **38,** 12302 (2013).

[14] J. D. Benck, Z. B. Chen, L. Y. Kuritzky, A. J. Forman and T. F. Jaramillo, ACS Catal., **2**, 1916 (2012).

[15] Y. H. Chang, C. T. Lin, T. Y. Chen, C. L. Hsu, Y. H. Lee, W. J. Zhang, K. H. Wei and L. J. Li, Adv. Mater., **25**, 756 (2013).